NASA Technical Memorandum 105978

Study of the Capacitance Technique for Measuring High-Temperature Blade Tip Clearance on Ceramic Rotors

John P. Barranger
Lewis Research Center
Cleveland, Ohio

March 1993

NASA

STUDY OF THE CAPACITANCE TECHNIQUE FOR MEASURING HIGH-TEMPERATURE BLADE TIP CLEARANCE ON CERAMIC ROTORS

John P. Barranger
National Aeronautics and Space Administration
Lewis Research Center
Cleveland, Ohio 44135

SUMMARY

Higher operating temperatures required for increased engine efficiency can be achieved by using ceramic materials for engine components. Ceramic turbine rotors are subject to the same limitations with regard to gas path efficiency as their superalloy predecessors. In this study, a modified frequency-modulation system is proposed for the measurement of blade tip clearance on ceramic rotors. It is expected to operate up to 1370 °C (2500 °F), the working temperature of present engines with ceramic turbine rotors. The design of the system addresses two special problems associated with nonmetallic blades: the capacitance is less than that of a metal blade, and the effects of temperature may introduce uncertainty with regard to the blade tip material composition. To increase capacitance and stabilize the measurement, a small portion of the rotor is modified by the application of 5-μm-thick platinum films. The platinum surfaces on the probe electrodes and rotor that are exposed to the high-velocity gas stream are coated with an additional 10-μm-thick protective ceramic topcoat. A finite-element method is applied to calculate the capacitance as a function of clearance.

INTRODUCTION

Ceramic materials are being considered for gas turbine engine components to achieve higher engine operating temperature and decreased cooling requirements. With regard to gas path efficiency, ceramic rotors are subject to the same limitations as their superalloy predecessors. Excess blade tip clearance allows a portion of the engine gas to flow over the blade tip without performing useful work. Moreover, insufficient clearance may cause interference that can jeopardize engine integrity.

Capacitance sensors have been used extensively to measure blade tip clearance (refs. 1 to 5). The present frequency-modulation (FM) system meets the needs of a wide class of gas turbine engines with superalloy rotors. The maximum working temperature for this system is 1095 °C (2000 °F).

In this study, a modified FM system is proposed for the measurement of blade tip clearance on ceramic rotors. It is expected to operate up to 1370 °C (2500 °F), the working temperature of present engines with ceramic turbine rotors.

Nonmetallic blades present two special problems: the blade capacitance is less than that of a metal blade, and the effects of temperature may introduce uncertainty with regard to the blade tip material composition. To increase the blade capacitance and stabilize the effects of temperature, a portion of the rotor is modified by the application of 5-μm-thick platinum films. The metal coating is applied to the blade tips and to connecting stripes that become part of the ground return path. The platinum surfaces on the probe electrodes and the rotor that are exposed to the high-velocity gas stream are coated with an additional 10-μm-thick protective ceramic topcoat.

The study showed that, for the purpose of determining the blade capacitance, the ceramic blade tip coated with the platinum is equivalent to an all-metal blade tip. Further, the higher resistance of the ground return path of the proposed system has only a minor impact on performance.

A finite-element method was used to determine the blade capacitance as a function of clearance. Calculations showed that the presence of the topcoat lowers the blade capacitance slightly.

The proposed system is intended for blade tip clearance measurements made during the component and full-scale testing phases of engine development. Large-scale vacuum facilities able to accommodate entire rotors are now available for metal film deposition. Moreover, thin-film thermocouples and heat flux gages can be applied concomitantly.

The NASA Lewis Research Center has an ongoing program to develop thin-film thermocouples on ceramic materials (ref. 6). The thermocouples are intended to have a lifetime of 50 hr or more and to be able to withstand temperatures up to 1500 °C (2730 °F). The results of this program are directly applicable to the proposed modified FM measurement system.

SUPERALLOY ROTOR SYSTEM DESCRIPTION

The present turbine clearance system described in this section is shown in figure 1. Designated a superalloy rotor system to distinguish it from that proposed for ceramic rotors, it consists of an electronics unit, a coaxial connecting cable, a probe termination, and a high-temperature capacitance probe. The electronics unit contains the FM oscillator electronics and the signal conditioner (ref. 5). The oscillator has an operating frequency in the range of 35 to 45 MHz and accommodates the high rotor speeds associated with small engines, the signals from which may have frequency components as high as 1 MHz. The signal conditioner demodulates the oscillator output and provides a signal suitable for the data acquisition unit. The capacitance probe is a high-temperature version of the probe described in reference 5.

In the capacitance probe installation (fig. 2), the clearance d is defined as the distance between the rotor blade tip and the probe face. This is also the distance to the shroud since the probe is shown mounted flush with the shroud. The probe may also be recessed slightly to avoid interference should the shroud abrade. The blade is electrically grounded through the shaft, bearings, case, etc. (The probe-to-shroud and probe-to-case attachments are not shown.)

The probe has coaxial construction: the inner electrode rod is separated from the outer electrode tube by a ceramic insulator. The electrodes are composed of a superalloy with a maximum working temperature of 1095 °C (2000 °F), a temperature which is consistent with the maximum gas temperature for many engines with superalloy turbine rotors.

The insulator is composed of alumina. Because the electrical properties of alumina change with temperature, the insulator is set back from the probe tip to minimize the effect of its temperature on the blade capacitance. Furthermore, setting back the insulator reduces the possibility of insulator surface contamination caused by combustion products such as soot and metal particles.

The metal bellows in the probe termination is preloaded in tension in order to apply a tensile force to the inner electrode. This arrangement prevents the inner electrode from extending into the gas stream as a result of thermal expansion effects.

Because the gas path temperature is very high and the probe length is not very long, there exists the possibility that the temperature outside the engine case is sufficiently high to weaken the spring action of the bellows and, further, cause deterioration of the nearby coaxial cable connector. When necessary, therefore, the probe termination is cooled to lower the temperature to acceptable levels.

Terminal pair 1-1′ represents the connection between the probe termination and the end of the coaxial cable. The capacitance C, looking into terminal 1-1′, can be thought of as the sum of the capacitance of the probe and the probe termination alone and the capacitance introduced by the presence of the blade. To visualize this concept, imagine that two blades with different clearances pass under the probe. The total capacitance for the two blades as a function of time t would be $C(t)$, as shown in figure 3. Making the probe diameter much smaller than the interblade spacing results in $C(t)$ becoming equal to the capacitance of the probe and the probe termination alone between blade pairs. Let this probe capacitance be called C_o. At the point of maximum capacitance

$$C_m = C_o + C(d) \tag{1}$$

where $C(d)$ is the blade capacitance and d is the clearance between the blade tip and the probe face. The value of $C(d)$ increases as d decreases and is usually very small, typically 1 pF or less.

HIGH-TEMPERATURE ROTOR MATERIALS

Nonmetallic blades present two special problems: the blade capacitance is less than that of metal blades, and the effects of temperature may introduce uncertainty with regard to the material composition of the blade tip. The smaller capacitance decreases the frequency deviation of the FM oscillator, thereby reducing the accuracy of the clearance measurement (ref. 5). For the accuracy of the calibration taken at room temperature to be maintained under the operating environment, the pertinent characteristics of the composition of the blade tip should not change with time or temperature. In order to address the composition problem, the physical and electrical properties of three types of rotor ceramics are discussed in the balance of this section.

The leading candidate for a rotor ceramic at the present time is silicon nitride Si_3N_4. Measurements made by the author at room temperature on rotor grade silicon nitride showed a blade capacitance of approximately 20 percent that of metal. Bulk silicon nitride has a dielectric constant (relative permittivity) of nearly 10 at its high density. This form of silicon nitride remains a dielectric up to at least 1370 °C (2500 °F). Practical materials, however, may not be such good dielectrics (see the appendix).

At elevated temperatures, oxygen reacts with the exposed surface to form a silica scale. In general, the scale is slow-growing protective oxide (ref. 7). At 1400 °C (2550 °F), however, the scale was visibly cracked from the crystallization of silica into cristobalite (ref. 8). Other mechanisms, such as engine thermal cycling and the presence of water vapor, may accelerate the rate of oxidation (ref. 7).

The morphology and chemical makeup of the scale is very complex. The presence of impurities or deliberate additions to the silicon nitride may form other chemical compounds such as silicates. In a study of the silicon nitride-based ceramic Si_3N_4: 2.3 MgO: 19.3 Nd_2O_2 (ref. 9), the oxide scale formed at 1300 °C (2370 °F) was porous and disrupted by voids that developed in the evolution of gaseous nitrogen. The bulk of the oxide scale layer was thought to be pure silica but was also found to be silicon rich, probably due to the silicate of neodymium. Because of its accelerated oxide growth, this material may not be a good candidate for a rotor application. This example does illustrate, however, how complex the nature of the blade tip can become.

Another impurity that may signal a change in the electrical properties of the blade tip is free silicon, which can occur as a result of manufacturing necessity. Silicon can have a wide range of conductivity from room to high temperature. Thus, when silicon is present, there exists an uncertainty with regard to the specific electrical characteristics of the blade tip.

Another ceramic proposed for rotors is silicon carbide SiC. Room temperature measurements made by the author on rotor grade silicon carbide showed a blade capacitance of approximately 60 percent that of metal. Unlike silicon nitride, however, it behaves electrically more like silicon than a dielectric. The high-temperature degradation of silicon carbide is similar in many ways to that of silicon nitride. Oxidation at high temperatures forms a cracked oxide scale (ref. 8).

A composite of silicon carbide fibers in a silicon nitride matrix is often proposed for future ceramic engines. One of the fibers being studied (ref. 10) has an overall diameter of 142 μm and an inner conductive carbon core 37 μm in diameter. Some smaller fibers (ref. 11) are monolithic polycrystalline types. The resultant composite structure may take the form of conducting fibers in a dielectric matrix.

The previous discussion points out the difficulty of precisely defining the high-temperature material characteristics and stability of three types of rotor ceramics: silicon nitride, silicon carbide, and a composite of silicon carbide fibers in a silicon nitride matrix. Without modifications, these rotors may introduce unacceptable clearance error into the measurement system.

PROPOSED CERAMIC ROTOR MEASUREMENT SYSTEM

The proposed system is designed to measure the blade tip clearance of gas turbine engines with ceramic rotors. The design is illustrated on a recently developed engine with ceramic components, the AGT101 (refs. 12 and 13). Monolithic silicon nitride is the rotor material for this engine; the hub is connected to a metal shaft via a ceramic-to-metal attachment. The maximum turbine inlet temperature is 1370 °C (2500 °F). The proposed system design is targeted at the rotor configuration and the temperature environment of the engine.

From the discussions in the previous sections, three issues emerge that impact the design of blade tip clearance systems with ceramic rotors: the expected turbine inlet temperature is higher than the maximum working temperature of the superalloy probe electrodes; the blade capacitance is less than that of metal blades; and the ceramic rotor materials do not have a stable, precisely defined composition.

For the purpose of the design, the stability of the measurement system is defined in terms of its running time. The system is intended for measurements made during the component and full-scale testing phase of engine development. Thus, a running time of at least 50 hr before recalibration is adequate.

To address the design issues, the probe electrode material was changed from a superalloy to platinum, and a small portion of the rotor was modified by the application of coatings. A metal coating, platinum film, was applied to all the blade tips. The blade tip coatings in turn were connected to narrow platinum stripes that traced a continuous path from the blade tips along the blade sides, joined together at the rotor hub, and finally connected to the metal shaft via the ceramic-to-metal attachment. The stripes were part of the blade tip ground return path. In addition to these modifications, platinum surfaces on the probe electrodes and rotor that are exposed to the high-velocity gas stream are coated with a protective alumina topcoat.

In the next three sections, key aspects of the design are discussed. The first addresses the question of conductor materials in high-temperature environments. The second deals with an issue that can impact performance: the resistance of the ground return path. In the last section, the blade capacitance is calculated by using the finite-element method.

HIGH-TEMPERATURE CONDUCTOR MATERIALS

Because of the high-temperature environment, special consideration is given to electrical conductor materials that are used both in the probe electrodes and the rotor coatings. From the point of view of electrical conductivity, some of the best candidate materials are the platinum group metals—platinum, rhodium, and iridium. Unfortunately, noble metals react with the oxygen in the high-temperature gas stream to form volatile oxides. The recession rate, or loss of metal, depends on, among other factors, the flow rate of gas past the metal. For platinum, the recession rate is 0.7 μm/hr at 1370 °C (2500 °F) when the test flow rate is 10 mm/sec (ref. 14). (The recession rate may be higher for turbine engines where typical blade tip speeds are hundreds of meters per second.) For the design running time of 50 hr, the total loss is 35 μm, a change in dimension inconsistent with precision measurements.

Another disadvantage of noble metals is their inability to resist erosion by the high-velocity gas stream. The soft metal surface is grooved by bits of hard metal and ceramic material and wears off in the form of fine shavings. The wear rate is unknown at the present time but could be of the same order of magnitude as the recession rate.

To overcome the aforementioned deficiencies, a protective topcoat is applied over the conductor. The coating material must be oxidation resistant to minimize recession and must be mechanically hard to resist erosion. Candidate materials are alumina Al_2O_3, hafnia HfO_2, and zirconia ZrO_2.

The thickness of the coating is a critical design parameter for both the conductor and the topcoat. The coatings should be thin in order to resist the interface debonding that arises from the mismatch of thermal coefficients of expansion. Narrow, thin conductive coatings, on the other hand, may compromise the system performance because of the resultant high electrical impedances. This question is addressed in the following section and in the appendix. Also, topcoats that are too thin may not provide adequate protection for the necessary running time.

Platinum was chosen as the probe electrode material because of its high ductility, easy workability, high melting point, and extensive solid solution possibilities with other metals. Platinum was also chosen as the rotor coating material because of its successful application as a thin film on ceramic substrates. With a protective topcoat of alumina, a platinum coating with a thickness of 5 μm was tested up to 1000 °C (1830 °F) (ref. 15). Platinum group thermocouples, 5 to 7 μm thick, were successfully sputtered and tested to temperatures above 1250 °C (2280 °F) (ref. 6). Based on these results, the platinum coating thickness for the rotor was set to 5 μm and the alumina topcoat thickness for the rotor and the probe tip was set to 10 μm. Because the hardness of aluminum oxide is nearly the same as that of silicon nitride, the erosion was not expected to be serious for the testing environment and running time.

GROUND RETURN PATH

In the measurement system for superalloy rotors, the blade is electrically grounded through the shaft, bearings, case, etc. For the proposed system, the conductive ground return path for the blade tip coating is through the stripe, shaft attachment, shaft, bearings, case, etc. Because the stripe has a higher resistance than the metal rotor, the ground return resistance is higher for the proposed system. The higher resistance impacts the following pertinent aspects of the ground return path: the equivalent shunt resistance and the electrical grounding of the blade tip. It is shown in this section that (1) the equivalent shunt resistance is larger than the minimum acceptable shunt resistance (ref. 5), and (2) the blade tip potential is nearly at ground potential. Thus, the higher resistance has only a minor impact on the performance of the proposed system.

The equivalent lumped-element network for the probe configuration and the ground return path (fig. 4) shows a capacitance between the inner electrode and the blade tip C_2 and a capacitance between the blade tip and the outer electrode C_3. The input admittance Y between the inner and outer electrodes is the admittance looking into terminal 1-1′ (fig. 2) in the presence of the blade less the admittance in the absence of the blade $j2\pi fC_o$ (fig. 3).

The ground return resistance R represents the resistance of the stripe from the blade tip to the shaft attachment. The resistance of the shaft attachment, shaft, bearings, case, etc. is assumed to be much smaller than R and is therefore neglected. Since the protective coating is a good dielectric (appendix), its effect is also neglected.

Because the coating thickness is small compared to the skin depth (appendix), the current density is nearly uniform and the resistance is therefore given by

$$R = \frac{L}{\sigma h W} \tag{2}$$

where σ is the conductivity, and L, h, and W are the total length, thickness, and width of the stripe, respectively. Setting $\sigma = 1.90\times10^6$ S/m or mhos/m (platinum at 1370 °C or 2500 °F), $L = 0.5$ m, $W = 1$ mm, and $h = 5$ μm, R becomes 53 Ω.

The input admittance Y is found from

$$Y = \frac{j2\pi fC_2\left(\frac{1}{R} + j2\pi fC_3\right)}{\frac{1}{R} + j2\pi f(C_2 + C_3)} \tag{3}$$

where f is the operating frequency. For a frequency of 45 MHz, a maximum value of C_2 of approximately 1 pF and a maximum value of C_3 of the same order of magnitude as C_2, equation (3) reduces to

$$Y = R(2\pi fC_2)^2 + j2\pi fC_2 \tag{4}$$

The input admittance is now equivalent to the parallel combination of the capacitance C_2 and the dissipative element $R(2\pi fC_2)^2$. By definition, C_2 is identified as the blade capacitance. The calculated reciprocal of the real part of Y yields a shunt resistance of 240×10^3 Ω, a value which is much larger than the minimum acceptable shunt resistance of 10×10^3 Ω (ref. 5).

The ratio of the blade tip potential to the inner electrode potential is

$$T = \frac{j2\pi fC_2}{\frac{1}{R} + j2\pi f(C_2 + C_3)} \tag{5}$$

For the values given above, the magnitude of T is less than 0.015. Thus, the blade tip is nearly at ground potential.

In some cases, a conductive ground return path may not be possible. This condition will occur if it becomes impractical to provide the stripes or if one or more parts of the return path, bearings, for example, are ceramic. The ground return resistance R (fig. 4 and eq. (3)) is now replaced by a stray impedance. If the quantity one divided by the stray impedance is small compared to $2\pi fC_3$, then the metal blade tip coating is considered a "floating" conductor and Y becomes $j2\pi fC_2C_3/(C_2 + C_3)$. Note that the blade capacitance has now been reduced by the factor $C_3/(C_2 + C_3)$. Besides the shortcoming of the reduced capacitance, this mode of operation is not recommended because it is difficult to determine the stability of the stray impedance under all operating conditions.

BLADE CAPACITANCE VIA THE FINITE-ELEMENT METHOD

An understanding of the system parameters that influence the blade capacitance is of critical importance to the design of the blade tip clearance system. Of particular interest are the effects of the probe and rotor dimensions and their respective materials. In order to calculate the value of the blade capacitance for all types of rotor materials and probe configurations, it would be convenient if a closed-form analytic solution existed. Unfortunately, such a solution does not exist for most practical geometries.

A procedure for adapting the finite-element method to the solution of electric field problems has been developed for the personal computer (PC) by Ansoft Corporation (refs. 16 and 17). The technique can solve two-dimensional planar and axisymmetric static field problems involving geometric objects that are perfect dielectrics or perfect conductors. Perfect dielectrics have a zero imaginary part of permittivity and perfect conductors have an infinite conductivity. It would seem, at first, that the technique can only be applied to cases with static fields and perfect materials. On the contrary, the method yields excellent results for situations where (1) time-varying fields meet the quasi-static approximation and (2) objects are good dielectrics or good conductors. This section shows that the proposed design conforms to these two constraints, thereby permitting the use of the finite-element method to calculate the blade capacitance.

Objects are entered by drawing the complete outline of the objects with their boundaries. Each object is designated a conductor or a dielectric with a specified dielectric constant. The protective topcoat is considered a separate object both on the blade and the probe. Only those portions of blade and the probe that contribute to the blade capacitance are simulated.

For the proposed probe tip configuration (fig. 5(a)), the blade has a rectangular cross section and is centered over the probe to simulate C_m (eq. (1)). This configuration has neither a planar nor an axisymmetric geometry; the fields are therefore not two dimensional. In spite of this limitation, useful results can be obtained when certain approximations are made. If the blade width (1 mm) is small compared to the inner electrode diameter (5 mm), the simplified configuration has a two-dimensional planar geometry (fig. 5(b)). This simplification forces the y-component of the electric field $E_y(z)$ to be zero for all z, which is equivalent to neglecting the fringe field in the y-direction. The line $z = 0$ is defined such that the discontinuity at the open end does not support a z-component of the field at this line. Thus, the field at $z = 0$ has only one component $E_x(0)$.

The two constraints that permit the use of the finite-element technique for the proposed design are now considered. The quasi-static approximation (ref. 18, p. 578) is easily met by the probe tip geometry; the physical dimensions are hundreds of times smaller than the wavelength corresponding to the 35- to 45-MHz range of frequencies. The analysis in the appendix shows that platinum, the probe electrode material, is considered a good conductor and that alumina, the material of the protective topcoat, is a good dielectric (dielectric constant $\varepsilon_r = 9.3$). The analysis also reveals that the platinum-coated silicon nitride blade tip is equivalent to an all-metal (good conductor) blade tip.

The inner electrode potential is arbitrarily set to 1 V and the outer electrode is set to 0 V, the ground potential. It was shown in equation (5) that the blade tip is nearly at ground potential. Thus, the blade can be considered an extension of the outer electrode.

The software that solves the field equations also contains a versatile calculator that includes the operations of vector dot product and integration. The capacitance can be defined in terms of these operations on the electric field vector $\boldsymbol{E}$ and the flux density $\boldsymbol{D}$ as

$$\frac{1}{2}CV^2 = \frac{1}{2}\int_v \boldsymbol{D} \cdot \boldsymbol{E}\, dx\, dy\, dz \tag{6}$$

where C is the capacitance, V is the voltage between the electrodes, and $dx\, dy\, dz$ is the volume element of the volume v. The energy balance expressed in equation (6) relates the energy stored in the capacitance to the integration of the energy distribution in the field throughout the volume. For the configuration in figure 5(b), the capacitance is found from

$$C = w\int_s \boldsymbol{D} \cdot \boldsymbol{E}\, dx\, dz \tag{7}$$

where V has been set to 1 V, w is the width of the blade, and the integration is now taken over the xz-plane s. The blade capacitance $C(d)$ (eq. (1)) is the difference between $C = C_m$ found with the blade and $C = C_o$ found without the blade.

The blade capacitance as a function of clearance was calculated for the blade tip composed of a good conductor but without the protective topcoat on either the blade tip or the probe tip (fig. 6(a)). This plot is applicable to both the superalloy and the proposed rotor with the conductive coating. When the blade tip and probe tip are coated with the protective dielectric topcoat, the resultant blade capacitance is slightly less (fig. 6(a)), particularly at the smaller clearances (fig. 6(b)). Moreover, these plots show that the presence of the topcoat influences the results, and the proposed system should therefore be calibrated after the topcoat has been applied.

The blade capacitance values for completely uncoated ceramic blades with dielectric constants of 5, 10, and 15 were also calculated. Figure 6(a) shows that ceramic rotors suffer from low blade capacitance.

CONCLUDING REMARKS

A modified frequency-modulation capacitance technique has been proposed for measuring blade tip clearance up to 1370 °C (2500 °F). Because of low-capacitance and oxidation effects, the ceramic rotor was modified by the addition of conductive and protective coatings. The necessary modifications are within the present capability of the aeronautics industry.

APPENDIX—COATED CERAMIC AND METAL BLADE EQUIVALENCE

The analysis in this appendix shows that, for the purpose of determining the blade capacitance, the silicon nitride blade tip coated with the 5-μm-thick platinum is equivalent to an all-metal blade tip. Also discussed are the influence of the thickness and the character of the coating, definitions of a good conductor, a good dielectric, and the skin depth.

The following analysis is similar to the perturbation method used in the study of transmission lines where the fields are between lossy boundaries (ref. 18, p. 437). A nearly uniform and nearly normal field pattern is assumed.

The blade tip of the proposed system (fig. 7(a)) is considered divided into two media separated by plane boundaries: medium 1, the platinum coating and medium 2, the silicon nitride blade. For the purposes of this analysis, it is not necessary to include the protective topcoat. The current I_1 traveling along the coating together with the current in the silicon nitride I_2, part of which may be conductive, must be supported by an electric field parallel to the surface. The value of this field at the surface E_o is given by (ref. 18, p. 152)

$$E_o = \frac{(I_1 + I_2)Z_i}{w} \tag{8}$$

where Z_i is the input impedance at the surface and w is the width of the blade.

The transmission line analogy (ref. 18, p. 286) is invoked to give the input impedance as

$$Z_i = \eta_1 \left(\frac{\frac{\eta_2}{\eta_1} + \tanh \gamma_1 h}{1 + \frac{\eta_2}{\eta_1} \tanh \gamma_1 h} \right) \tag{9}$$

where η_1 and η_2 are the intrinsic impedances of media 1 and 2, respectively, γ_1 is the propagation constant of medium 1, and h is the coating thickness. For a conductor, the intrinsic impedance is

$$\eta = \sqrt{\frac{\mu_o}{\varepsilon' \left(1 + \frac{\sigma}{j2\pi f \varepsilon'} \right)}} \tag{10}$$

and the propagation constant is

$$\gamma = j2\pi f \sqrt{\mu_o \varepsilon' \left(1 + \frac{\sigma}{j2\pi f \varepsilon'} \right)} \tag{11}$$

where μ_o is the permeability of free space ($4\pi\times10^{-7}$ H/m), $\varepsilon' = \varepsilon_o\varepsilon_r$ is the permittivity with ε_o the permittivity of free space (8.85×10^{-12} F/m) and ε_r the dielectric constant (ref. 18, p. 280), σ is the electrical conductivity, and f is the operating frequency.

A good conductor is now defined as one in which

$$\frac{\sigma}{2\pi f\varepsilon'} >> 1 \tag{12}$$

For a good conductor, η and γ simplify to

$$\eta = \frac{1 + j}{\sigma\delta} \tag{13}$$

$$\gamma = \frac{1 + j}{\delta} \tag{14}$$

where δ is the skin depth and is defined by

$$\delta = \sqrt{\frac{1}{\mu_o\pi f\sigma}} \tag{15}$$

Most metals qualify as good conductors at a frequency of 45 MHz. For medium 1, $\sigma_1 = 1.90\times10^6$ S/m (platinum at 1370 °C or 2500 °F), and the quantities representing equations (13) to (15) become $\eta_1 = (1 + j)9.7\times10^{-3}$ Ω, $\gamma_1 = (1 + j)1.8\times10^4$ Np/m, and $\delta_1 = 54$ μm, respectively.

For a dielectric, the term $\sigma/2\pi f$ in equations (10) and (11) is replaced by the imaginary part of permittivity ε''. A good dielectric is now defined as one in which

$$\frac{\varepsilon''}{\varepsilon'} = \tan\delta << 1 \tag{16}$$

where tan δ is called the loss tangent. High purity (≥99 percent) alumina meets the criterion of equation (16) up to at least 1370 °C (2500 °F). Measurements made on some samples of silicon nitride, however, show loss tangents of 0.22 at 1090 °C (1995 °F) (ref. 19). Thus, silicon nitride should be considered a lossy dielectric rather than a good dielectric at high temperatures and I_2, indeed, contains a conductive component. Using tan $\delta = 0.30$ (estimated) and $\varepsilon_r = 7.0$, the wave impedance of this substrate becomes complex and has the value $\eta_2 = 140 + j\,20$ Ω. With $h = 5$ μm, calculation of the input impedance (eq. (9)) yields the real value $Z_i = 0.11$ Ω.

For the coated blade tip to be electrically equivalent to the all-metal blade, it must be equivalent both in the case of current and voltage. In the former case, the current leaving the blade tip is required to be entirely in the metal for both configurations. This requirement can be satisfied if the inequality

$$\left|\frac{I_2}{I_1}\right| << 1 \tag{17}$$

is met, thereby identifying the current leaving the all-metal blade tip as I_1 (fig. 7(b)). Because the coating thickness h is small compared to the skin depth δ, the parallel electric field at the interface of mediums 1 and 2 is nearly E_o. Thus the inequality

$$\left|\frac{Z_i}{\eta_2 - Z_i}\right| << 1 \tag{18}$$

is equivalent to (17). From the previously given values, the lefthand side of (18) is 7.8×10^{-4} and the current requirement is satisfied.

In the case of the voltage equivalence, the voltage drop along the current path is to be the same for both configurations. This can be achieved if the voltage drop along the blade tip length ℓ in the direction of E_o is required to be small compared to the voltage drop across the gap clearance d in the direction of E. This requirement can be satisfied if the inequalities (17) and

$$\left|\frac{E_o \ell}{Ed}\right| << 1 \tag{19}$$

are met, thereby identifying the electric field across the all-metal blade tip gap as E (fig. 7(b)). The voltage Ed across the gap is now given by

$$Ed = \frac{I_1}{j2\pi f C(d)} \tag{20}$$

where $C(d)$, as before, is the blade capacitance. The criterion of (19) is equivalent to

$$\left|j2\pi f C(d) Z_i \frac{\ell}{w}\right| << 1 \tag{21}$$

where (17) has been applied to equation (8). For $C(d)$ = 1 pF, ℓ = 5 mm, and w = 1 mm, the lefthand side of (21) has a value of 1.6×10^{-4}. Thus, the silicon nitride blade tip with the 5-μm-deep platinum coating is equivalent to an all-metal blade tip for the purpose of determining blade capacitance. Note that this is true even though the coating thickness is less than 10 percent of the skin depth.

REFERENCES

1. Scotto, M.J.; and Eismeier, M.E.: High-Speed Noncontacting Instrumentation for Jet Engine Testing. J. Eng. Power, vol. 102, no. 4, Oct. 1980, pp. 912–917.

2. Loftus, P.: A Review of Non-Contacting Displacement Measurement Techniques Used to Monitor the Movement of Rotor Blades in Gas Turbine Aero Engines. Report PNR90457, Rolls-Royce Ltd., Derby, England. Presented at the Test and Transducer Conference, Oct. 1987.

3. Knoell, H.; and Ding, K.: Tip Clearance Measurement in Modern Compressor Components. Advanced Instrumentation for Aero Engine Components, AGARD CP–399, 1986, pp. 29–1 to 29–10.

4. Paulon, J.: Influence et Mesure du Jeu Bout D'Aubes dans les Turbomachines (The Effect and Measurement of Blade Tip Clearance in Turbomachinery). Heat Transfer and Cooling in Gas Turbines, AGARD CP–390, 1985, pp. 34–1 to 34–8.

5. Barranger, J.P.: Low-Cost FM Oscillator for Capacitance Type of Blade Tip Clearance Measurement System. NASA TP–2746, 1987.

6. Holanda, R.: Development of Thin Film Thermocouples on Ceramic Materials for Advanced Propulsion System Applications. To be published as NASA TM–106017, 1993.

7. Jacobson, N.S.: High Temperature Durability Considerations for HSCT Combustor. NASA TP–3162, 1992.

8. Fox, D.S.: Oxidation Kinetics of CVD Silicon Carbide and Silicon Nitride. Ceram. Eng. Sci. Proc., vol. 13, no. 9–10, Sept.–Oct. 1992, pp. 836–851.

9. Pomeroy, M.; and Hampshire, S.: Oxidation Processes in Silicon-Nitride-Based-Ceramics. Ceramic Materials Research: Proceedings of Symposium A on Ceramic Materials Research of the E–MRS Spring Conference, R.J. Brook, ed., Elsevier, New York, 1989, pp. 389–394.

10. DiCarlo, J.A.: High Performance Fibers for Structurally Reliable Metal and Ceramic Composites. NASA TM–86878, 1984.

11. Lipowitz, J., et al.: Silicon Carbide Fibers From Methylpolysilane (MPS) Polymers. Ceram. Eng. Sci. Proc., vol. 9, July–Aug. 1988, pp. 931–942.

12. Carruthers, W.D.; and Smith, J.R.: Ceramic Component Development for the AGT101 Gas Turbine Engine. Ceram. Eng. Sci. Proc., vol. 5, May–June 1984, pp. 350–368.

13. Richerson, D.W.: Evolution in the U.S. of Ceramic Technology for Turbine Engines. Am. Ceram. Soc. Bull., vol. 64, Feb. 1985, pp. 282–286.

14. Kaplan, R.B.; Fry, V.; and Harding, J.T.: Oxidation Protection of Rhenium Thrusters for 2480 K Cyclic Operation by Means of CVD Coatings. NAS3–24868, July 1986.

15. Prakash, S.; Budhani, R.C.; and Bunshah, R.F.: Development of Thin Film Temperature Sensors for High Performance Turbo-Jet Engines. Mater. Res. Bull., vol. 23, no. 2, Feb. 1988, pp. 187–195.

16. Cendes, Z.J.: Unlocking the Magic of Maxwell's Equations. IEEE Spectrum, vol. 26, no. 4, Apr. 1989, pp. 29–33.

17. Cendes, Z.J.; Shenton, D.; and Shahnasser, H.: Magnetic Field Computation Using Delaunay Triangulation and Complementary Finite Element Methods. IEEE Trans. Magnet., vol. MAG19, no. 6, Nov. 1983, pp. 2551–2554.

18. Ramo, S.; Whinnery, J.R.; and Van Duzer, T.: Fields and Waves in Communication Electronics. Second ed., John Wiley & Sons, New York, 1984.

19. Messier, D.R.; and Wong, P.: Silicon Nitride: A Promising Material for Radome Applications. Report AMMRC TR 74–21, Army Materials and Mechanics Research Center, Watertown, MA, 1974.

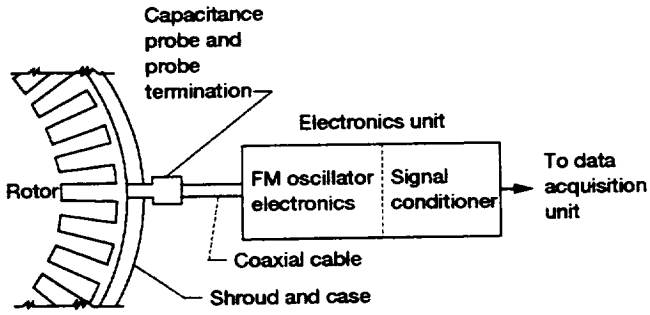

Figure 1.—Blade tip clearance measurement system.

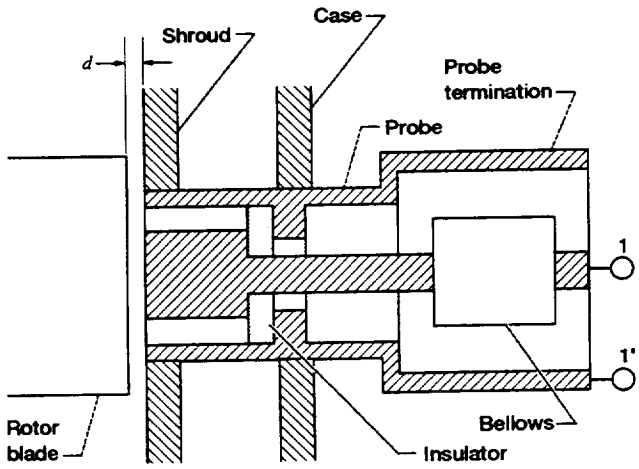

Figure 2.—Capacitance probe installation.

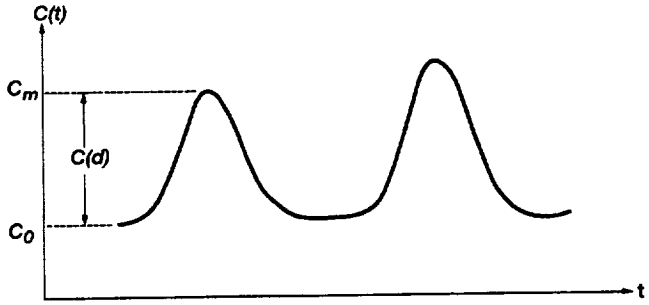

Figure 3.—Capacitance as function of time for two blades to pass under probe tip.

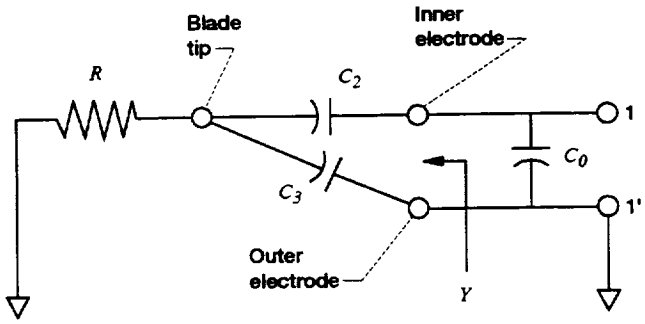

Figure 4.—Equivalent lumped-element network for ground return path.

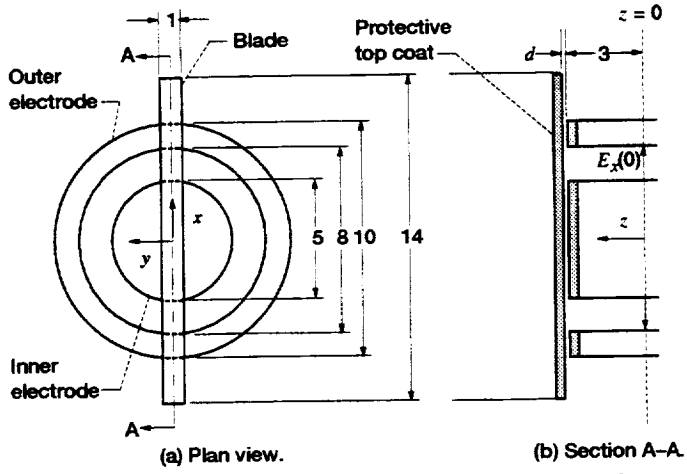

Figure 5.—Blade and probe tip configuration (All dimensions are in mm; topcoat thickness,10 μm.)

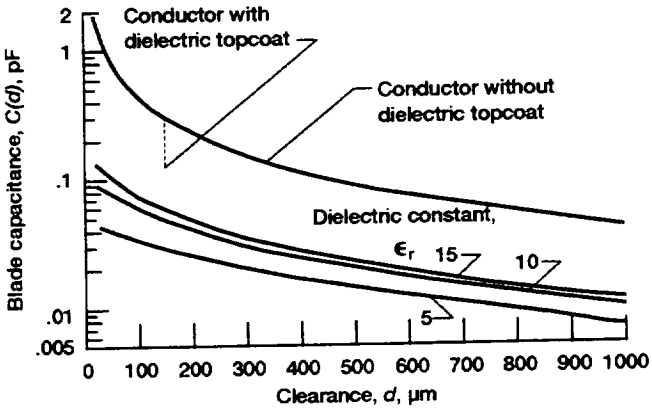

(a) Blade capacitance.

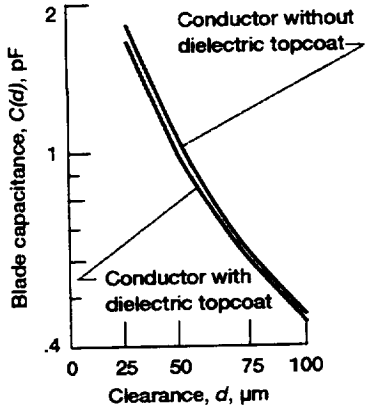

(b) Expanded scale of (a).

Figure 6.—Blade capacitance as a function of clearance.

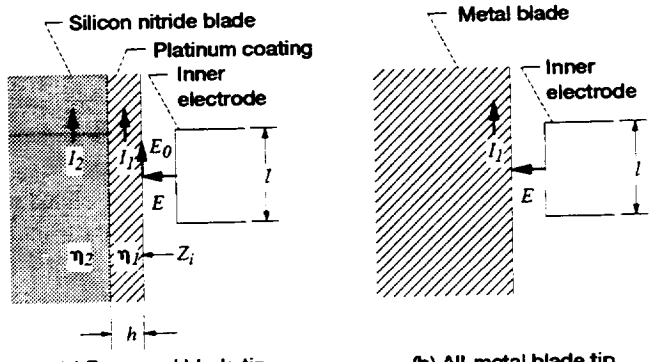

(a) Proposed blade tip.

(b) All-metal blade tip.

Figure 7.—Blade tip and inner electrode configurations.

REPORT DOCUMENTATION PAGE

Form Approved
OMB No. 0704-0188

1. AGENCY USE ONLY (*Leave blank*)	2. REPORT DATE	3. REPORT TYPE AND DATES COVERED
	March 1993	Technical Memorandum

4. TITLE AND SUBTITLE

Study of the Capacitance Technique for Measuring High-Temperature Blade Tip Clearance on Ceramic Rotors

5. FUNDING NUMBERS

WU-510-01-50

6. AUTHOR(S)

John P. Barranger

7. PERFORMING ORGANIZATION NAME(S) AND ADDRESS(ES)

National Aeronautics and Space Administration
Lewis Research Center
Cleveland, Ohio 44135-3191

8. PERFORMING ORGANIZATION REPORT NUMBER

E-7502

9. SPONSORING/MONITORING AGENCY NAMES(S) AND ADDRESS(ES)

National Aeronautics and Space Administration
Washington, D.C. 20546-0001

10. SPONSORING/MONITORING AGENCY REPORT NUMBER

NASA TM-105978

11. SUPPLEMENTARY NOTES

Responsible person, John P. Barranger, (216) 433-3642.

12a. DISTRIBUTION/AVAILABILITY STATEMENT

Unclassified - Unlimited
Subject Category 07

12b. DISTRIBUTION CODE

13. ABSTRACT ***(Maximum 200 words)***

Higher operating temperatures required for increased engine efficiency can be achieved by using ceramic materials for engine components. Ceramic turbine rotors are subject to the same limitations with regard to gas path efficiency as their superalloy predecessors. In this study, a modified frequency-modulation system is proposed for the measurement of blade tip clearance on ceramic rotors. It is expected to operate up to 1370 °C (2500 °F), the working temperature of present engines with ceramic turbine rotors. The design of the system addresses two special problems associated with nonmetallic blades: the capacitance is less than that of a metal blade and the effects of temperature may introduce uncertainty with regard to the blade tip material composition. To increase capacitance and stabilize the measurement, a small portion of the rotor is modified by the application of 5-μm-thick platinum films. The platinum surfaces on the probe electrodes and rotor that are exposed to the high-velocity gas stream are coated with an additional 10-μm-thick protective ceramic topcoat. A finite-element method is applied to calculate the capacitance as a function of clearance.

14. SUBJECT TERMS

Turbomachinery; Bladetips; Ceramics; Capacitance

15. NUMBER OF PAGES

18

16. PRICE CODE

A03

17. SECURITY CLASSIFICATION OF REPORT	18. SECURITY CLASSIFICATION OF THIS PAGE	19. SECURITY CLASSIFICATION OF ABSTRACT	20. LIMITATION OF ABSTRACT
Unclassified	Unclassified	Unclassified	

National Aeronautics and
Space Administration

Lewis Research Center
Cleveland, Ohio 44135

FOURTH CLASS MAIL

ADDRESS CORRECTION REQUESTED

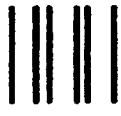

Official Business
Penalty for Private Use $300

Postage and Fees Paid
National Aeronautics and
Space Administration
NASA 451